Exchanging Bandwidth With Aperture Size in Wireless Indoor Localization - Or Why 5G/6G Systems With Antenna Arrays Can Outperform UWB Solutions

ERIK SIPPEL , **JOHANNA GEISS** **(Student Member, IEEE), STEFAN BRÜCKNER,**
PATRICK GRÖSCHEL **(Student Member, IEEE), MARKUS HEHN** **(Student Member, IEEE),**
AND MARTIN VOSSIEK **(Fellow, IEEE)**

Institute of Microwaves and Photonics, Friedrich-Alexander University Erlangen-Nuremberg, Erlangen 91058, Bavaria, Germany

CORRESPONDING AUTHOR: ERIK SIPPEL (e-mail: erik.sippel@fau.de)

ABSTRACT The localization of wireless devices in indoor scenarios presents a major challenge because of multipath propagation. Hence, the majority of the research community has focused on increasing the available bandwidth of localization systems, leading to the emergence of the ultra wide band (UWB) radar. However, the hardware implementation of UWB transceivers is challenging itself and, hence, their utilization in commercial low-cost wireless devices is not to be expected in the near future. Hence, instead of evaluating frequency dependent phases via UWB, the measurement of spatially distributed phases represents a valuable alternative. Therefore, this article presents a comparison of phase-difference-of-arrival (PDOA) and time-of-arrival (TOA) systems. For this purpose, we compare the measurement sensitivity, the effects of multipath propagation, and the hardware complexity. Based on the results, the applicability of typical position estimators is discussed. Thereby, we argue that PDOA-based localization with large receiver arrays appears to be the better choice to localize wireless devices, because it enables highly accurate positioning using narrow band signals without elaborated transmitter–receiver synchronization. To validate this, indoor localization measurements are presented and compared with UWB results in extant literature.

INDEX TERMS Radar, indoor localization, antenna array, ultra wide band, 5G, massive MIMO, Kalman filter.

I. INTRODUCTION

Nowadays, wireless localization systems are used in various applications, such as navigation, industrial automation, automotive radar, and service systems in for example hospitals or museums [1]. However, particularly in indoor and numerous urban scenarios, accurate localization represents a major challenge, because multipath propagation degrades the localization accuracy [2]. In particular, the localization of consumer electronic devices such as mobile phones within established communication standards is both of outstanding importance and rather challenging [3].

To collect information about a transmitter's position, different operation principles are possible [4]. The simplest principle measures the receive-signal strength (RSS), which decreases with increasing transmitter-receiver distance. Unfortunately, the constructive and destructive superposition of multipath propagation results in strong variations of the RSS and, hence, the localization accuracy is poor [5].

The distance estimation accuracy can be improved by measuring the wave's time-of-arrival (TOA) between the emission of the transmitter and reception of the receiver. For this purpose, a transmitter-receiver synchronization is necessary [6].
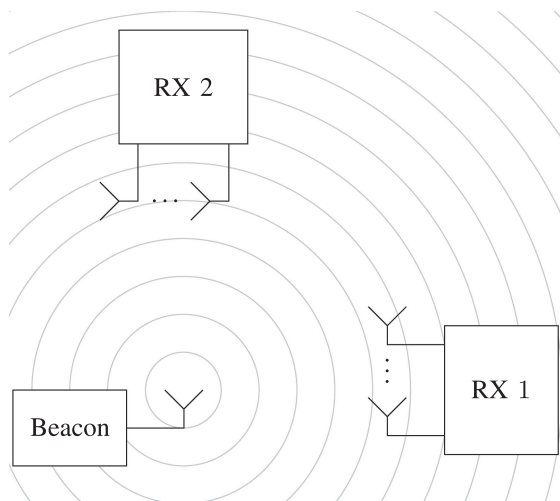
FIGURE 1. Illustration of the measurement environment, consisting of two receivers, which can either be used for TOA or PDOA measurements.

Alternatively, the time-difference-of-arrival (TDOA) can be evaluated using several synchronized receivers [7]. Most often, the TOA or TDOA is measured either using frequency-modulated-continuous-wave (FMCW) [8] or impulse-based systems [9]. Basically, TOA systems evaluate the frequency-dependent phase difference of a time delay. Thus, the localization accuracy depends strongly on the used bandwidth and therefore, ultra wide band (UWB) systems are employed in an attempt to increase the bandwidth as much as possible [7], [10]–[16]. In doing so, UWB systems both attempt to increase the measurement sensitivity and separate the line-of-sight (LOS) from the multipath propagation. Fig. 1 depicts an exemplary measurement environment with one beacon and two receivers. Here, TOA measurements provide horizontal beacon position information via receiver (RX) 1 and vertical position information via RX 2. Hence, by combining the measurements of several receivers via multilateration, the beacon's position can be estimated, as in [7].

Instead of evaluating the frequency-dependent phase relationship, spatially distributed phases at each receiver can be evaluated. This measurement concept is a well known one from the field of interferometry [17], particularly in terms of synthetic aperture radar (SAR) [18], [19]. However, SAR performs a coherent phase evaluation of multiple successive measurements, which is not possible for incoherent beacons. Hence, phase-difference-of-arrival (PDOA) systems evaluate the relative phase relation of impinging waves. For this purpose, spatially distributed measurements at coherently evaluated antennas within antenna arrays are evaluated [20]. Here, the transmitter's signal can be arbitrarily modulated and, hence, PDOA systems enable localization within common narrow band communication standards. Assuming the impinging wave to be plane, the angle-of-arrival (AOA) can be estimated at each array in an interferometric manner [21]–[23], in which the angle estimation accuracy depends on the positions of the RX antennas [24]. In Fig. 1, PDOA measurements

provide information on the vertical beacon position via RX 1 and on the horizontal position via RX 2. Therefore, the beacon's position can be estimated via multi-angulation [25].

Hence, PDOA and TOA systems provide fairly similar information regarding the beacon's position, when RX1 and RX2 are exchanged in Fig. 1, but their measurement accuracy depends on different system parameters. Therefore, for an indoor localization system, either a PDOA or a TOA system is the better choice, depending on the environmental conditions as well as the receiver's geometry and bandwidth. In order to evaluate the accuracy of AOA and TOA systems, their geometric dilution of precision and Cramer-Rao bounds were studied in [26]–[29]. However, the investigations assume AOA and TOA measurements, which are corrupted by zero-mean uncorrelated normally distributed errors, which is not valid for the PDOA based AOA estimations [30] and TOA in indoor environments [2], [7]. In order to enable fast accurate sensor fusion and the incorporation of movement statistics, commonly recursive filters estimate the position of the beacon by evaluating the raw measurement [31], [32]. Since the exact measurement errors for arbitrary indoor environments are difficult to model, the filters commonly assume uncorrelated normally distributed noise. Hence, standard indoor localization systems fundamentally violate these conditions.

Therefore, the main contribution of this paper is a thorough assessment of PDOA and TOA based localization systems with respect to their measurement sensitivity, resistance against multipath propagation, hardware implementation complexity, and their interaction in 3D position estimation filters. For this purpose, in Section II the measurement sensitivity of PDOA and TOA systems is studied using a far field assumption, which yields an easily interpretable rule of thumb for the direct comparison of PDOA and TOA systems, depending on the environment and the receivers' bandwidth and size. In comparison to wide band TOA systems, whose implementation is challenging and often limited due to governmental restrictions, narrow PDOA systems with large apertures can be easily implemented. However, the indoor localization with large arrays violates the far field assumption and, hence, the receivers evaluate circular instead of plane waves. As a favorable consequence, the wave forms of the LOS and the multipath propagation differ and, thus, the degradation of the 3D position estimation due to multipath propagation reduces, which is discussed in Section III. In Section IV, the established relationships are used to assess the applicability of the TOA and PDOA measurement principles with respect to the assumptions of established 3D position estimators, that are receivers at exactly known positions, which are impaired by zero mean uncorrelated normally distributed noise. Here, PDOA localization systems appear to be the better choice for the indoor localization of wireless devices, particularly because no elaborated hardware is necessary at the transmitter. Hence, the common trend of increasing the antenna number in communication systems, as within the massive multiple-input multiple-output (MMIMO) systems in 5G [33], [34] or particularly 6G [35]–[37], will enable highly accurate
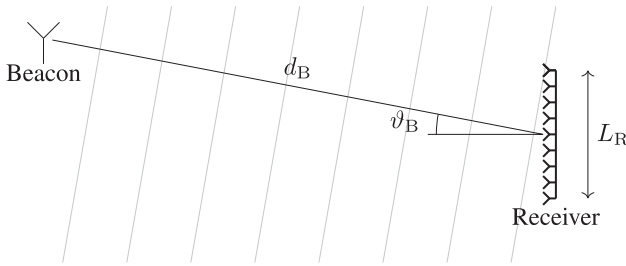
FIGURE 2. Illustration of the assumed measurement scenario used for comparison of PDOA and TOA. The array of size L_R receives a plane wave from the angle ϑ_B, emitted by a beacon in distance d_B.

PDOA-based user localization without the synchronization efforts of UWB measurements and by solely evaluating the communication signals. To validate our TOA-PDOA assessment, PDOA indoor localization results using the holographic extended Kalman filter (HEKF) [38] are presented and compared to the UWB literature in Section V.

Notation: In this paper, $\vec{(\cdot)}$ represents a vector and matrices are denoted in bold letters. $\arg(\cdot)$ evaluates the phase of a complex number and $|\cdot|$ the absolute value. The conjugate of a complex number is calculated by $(\cdot)^*$. A normal distribution with mean μ and variance σ^2 is denoted as $\mathcal{N}(\mu, \sigma^2)$. To map the ambiguous phase φ to $(-\pi, \pi]$,

$$\text{mod}'_{2\pi}(\varphi) = \begin{cases} \text{mod}_{2\pi}(\varphi) & \text{if } \text{mod}_{2\pi}(\varphi) \leq \pi \\ \text{mod}_{2\pi}(\varphi) - 2\pi & \text{if } \text{mod}_{2\pi}(\varphi) > \pi \end{cases}. \quad (1)$$

is used.

II. COMPARISON OF MEASUREMENT SENSITIVITY
In this section, the measurement sensitivity of PDOA and TOA systems is compared with respect to a beacon position change, thereby yielding an easily interpretable rule of thumb. For this purpose, the configuration illustrated in Fig. 2 is examined. Generally, a continuous wave signal (CW), which is emitted by the beacon, can be described at a distance d as

$$s(f, d) = A_B \frac{1}{d} e^{-j2\pi \frac{f}{c_0} d}, \quad (2)$$

where A_B denotes the complex valued unknown beacon phase and amplitude, f the frequency, and c_0 the speed of light [39]. The signal is received by a receiver in a distance d_B. A TOA measurement determines information regarding the position of the beacon by evaluating the relative phases for different frequencies f within a limited bandwidth B, thereby yielding information regarding the distance d_B. Note that this is valid independent of the exact radar implementation. Since the maximal measurement sensitivity is given by evaluating the phases at the maximally distant frequencies, $f_0 - B/2$ and $f_0 + B/2$, where f_0 denotes the radar's center frequency, the relevant phase difference is evaluated as

$$\Delta\varphi_{TOA} = \arg(s(f_0 - B/2, d_B)) - \arg(s(f_0 + B/2, d_B))$$

$$= \frac{2\pi}{c_0} d_B B. \quad (3)$$

Note that the phase difference is 2π ambiguous in general, which can be ignored here to discuss the measurement sensitivity. In order to evaluate the measurement sensitivity regarding a beacon position change in the range direction, the derivative of (3) is calculated, thereby yielding

$$\frac{\text{d}\Delta\varphi_{TOA}}{\text{d}d_B} = \frac{2\pi}{c_0} B. \quad (4)$$

Hence, the measurement sensitivity of TOA systems is solely influenced by the bandwidth and therefore, UWB localization systems continuously attempt to increase the available bandwidth.

In comparison, PDOA systems evaluate the relative phase for different receiver antenna positions. The measurement sensitivity is maximized by evaluating the phase difference between the most distant antennas. Assuming the receiver to be a linear array of aperture size L_R and the beacon to be in the far field of the array [40], the impinging wave can be fully characterized via a plane wave that arrives from angle ϑ_B, with respect to the horizontal axis, as depicted in Fig. 2. Then, the difference of the wave's traveled distance at the array's outer antennas is $\Delta d = \sin(\vartheta_B) L_R$. An evaluation of the emerging phase difference at the array's outer antennas yields

$$\Delta\varphi_{PDOA} = \arg(s(f_0, d_B - \Delta d/2) - \arg(s(f_0, d_B + \Delta d/2))$$

$$= \frac{2\pi}{c_0} f_0 L_R \sin(\vartheta_B). \quad (5)$$

Here, the maximal sensitivity, given by the derivative of (5), is yielded for $\vartheta_B = 0$. In this case, in contrast to a TOA evaluation, a beacon position change, x, orthogonal to the wave's direction of propagation and, hence, parallel to the array for $\vartheta_B = 0$ can be detected. Using a small-angle approximation for $\vartheta_B \approx \frac{x}{d_B}$, the maximum measurement sensitivity with respect to a beacon position change is approximated by

$$\frac{\text{d}\Delta\varphi_{PDOA}}{\text{d}x} \approx \frac{2\pi}{c_0} f_0 \frac{L_R}{d_B}. \quad (6)$$

Hence, the PDOA localization accuracy is influenced by the operating frequency because it is directly proportional to the phase sensitivity and the relative aperture size with respect to the beacon distance $\frac{L_R}{d_B}$. Comparing (4) and (6) enables to define an equivalent bandwidth for a PDOA system as

$$B_{PDOA,eq} = f_0 \frac{L_R}{d_{max}}, \quad (7)$$

where d_{max} is an approximate value for the maximal measurement distance. Hence, (7) enables a direct comparison of arbitrary localization systems using the TOA bandwidth B and the equivalent bandwidth $B_{PDOA,eq}$ of PDOA localization systems. Assuming that both systems operate in the same frequency band, that is the usage of the same center frequency f_0, (7) can be reordered, thereby indicating that a PDOA system can be assumed to outperform a TOA system whenever the relative array size is greater than the relative bandwidth, as

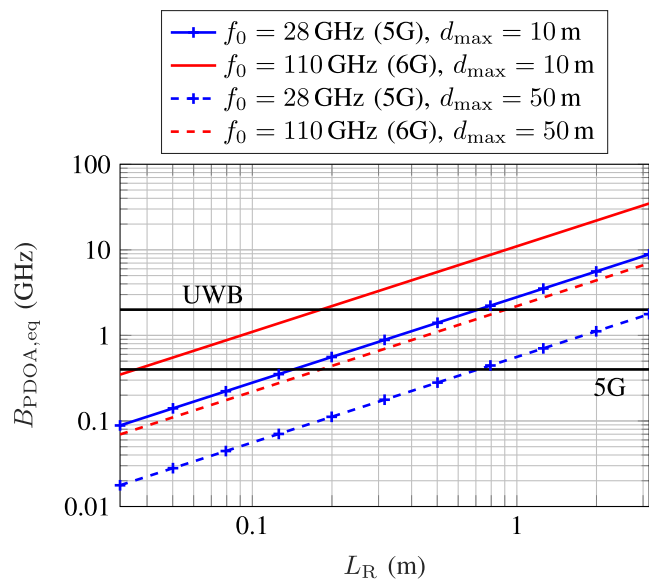$$\frac{L_R}{d_{max}} > \frac{B}{f_0}. \quad (8)$$

FIGURE 3. Illustration of the relationship between TOA and PDOA localization systems. The dashed and dashed dotted lines indicate the equivalent bandwidths $B_{\mathrm{PDOA,eq}}$ of hypothetical 5G and 6G systems of indoor localization systems with maximal distances of 10 m and 50 m depending on the aperture size, L_{R}. Further, the bandwidths of different established wireless systems are also depicted.
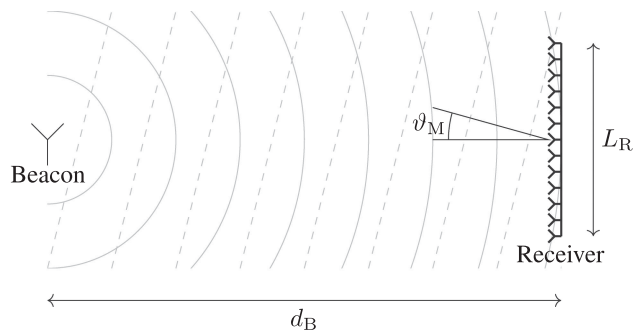

FIGURE 4. Illustration of the assumed measurement setup to discuss the decorrelation properties of circular waves. The array of size L_{R} receives a circular wave, emitted by the beacon at distance d_{B}, and a plane multipath wave, which impinges from ϑ_{M}.

On the other hand, the beacon was assumed to be located directly in front of the array and, hence, the sensitivity will be slightly less in most situations. On the other hand, a 3D localization within a room requires several receiving arrays and, therefore, the beacon will most often be located closer than $d_{\max}$ to certain receivers. Further, in a 3D localization system, one PDOA receiver can collect information in two angular directions, while a TOA receiver can only collect information in range direction. Overall, (7) provides an easy rule of thumb for the circumstances, in which a PDOA localization system outperforms a TOA localization system. Since a TDOA evaluation cannot outperform a TOA evaluation within the same error-free system setup, the developed relationship is similarly applicable.

To illustrate the relationship between TOA and PDOA localization, Fig. 3 shows the equivalent bandwidth of a 28 GHz and a 110 GHz wireless PDOA localization system, which correspond to hypothetical 5G and 6G indoor communication systems, in a 10 m and a 50 m environment as a function of the aperture size L_{R}. For comparison, the maximally available 5G user bandwidth $B_{5\,\mathrm{G}} = 400$ MHz and the bandwidth of a typical UWB system with $B_{\mathrm{UWB}} = 2$ GHz are plotted. According to (7), the equivalent bandwidth of a PDOA system decreases with increasing beacon distance and increases with increasing operating frequency and aperture size. Consequently, within the considered wireless systems, the bandwidth of every TOA system can be outperformed by sufficiently increasing the aperture size L_{R}. For example, within the 5G communication standard in a 10 m office, a PDOA system with aperture size $L_{\mathrm{R}} > 14.3$ cm is sufficient to outperform a 5G TOA

measurement, thereby eliminating the necessity for time synchronization.

To enable highly accurate TOA positioning, the UWB band of 3.1 GHz-10.6 GHz provides a bandwidth of 7.5 GHz. However, while the relative aperture size in (8) can be easily increased, systems with a high relative bandwidth cause implementational issues. Hence, strong scientific effort has been spent to advance UWB radars [10], [13]–[16]. To be able to combine the information of several UWB radars to a 3D position, all receivers are assumed to be fully modeled by a fixed location, which represents the antenna position. Hence, antennas are necessary, which combine a constant behavior for all angular directions and a high relative bandwidth. Generally, small antennas, which could be easily described via one fixed 3D receiver position, are fundamentally limited in their achievable bandwidth, unless they become disproportionately inefficient [41]–[43]. Hence, UWB antennas typically become physically large [39], [44]. Unfortunately, then the antenna's phase centers and transfer functions become direction-dependent [12], [45]–[47], which contradicts the requirement of a constant angular behavior. In contrast to UWB radars, PDOA localization systems do not require large bandwidths and, therefore, the required constant angular behavior is easily achievable.

Thus far, the calculations were performed in the far field domain, which is only an approximation but provides intuitive formulas. However, the far field approximation is not valid for large arrays in indoor environments. On the one hand, the reception of circular waves slightly decreases the measurement sensitivity. On the other hand, the localization within near field of the array helps to suppress the effects of multipath propagation, which will be discussed in the next section.

III. MULTIPATH PROPAGATION PROPERTIES OF CIRCULAR WAVES IN LOCALIZATION SYSTEMS

In this section, the effect of multipath propagation on indoor localization is discussed for TOA and PDOA systems. In this process, the advantage of antenna arrays, which measure within their near field, are discussed in an heuristic manner. The assumed environment is depicted in Fig. 4, consisting of

a receiver, which is illuminated by a beacon located in front of the receiver at $\vartheta_B = 0$. Again, (2) is used for LOS propagation with distance d_B. Further, we assume a multipath propagation signal to arrive as a plane wave from ϑ_M with distance d_M, where $d_M > d_B$ holds. Thereby, the plane wave assumption is justifiable, because the path of the multipath propagation is longer than the LOS. Note that multipath propagation is most often described via several impinging plane waves [48]. However, in this study, we only discuss the interaction of the LOS with a single multipath, because the effects superpose for more complex environments. Generally, the multipath propagation might influence the localization in two ways. First, the multipath propagation signal might falsely be detected as the LOS, thereby severely degrading the localization. However, this effect can easily be avoided within recursive filters. Second, the multipath propagation might distort the LOS signal's evaluation, which is examined in the following account. First, a TOA system is considered, where the receive signal is given by

$$s_R(f) = s_{LOS}(f) + s_M(f)$$
$$= A_{LOS} e^{-j2\pi \frac{f}{c_0} d_B} + A_M e^{-j2\pi \frac{f}{c_0} d_M}, \quad (9)$$

where $A_{LOS} = A_B/d_B$ and A_M is the complex receive amplitude of the multipath propagation. Since every least squares position estimation is essentially performed by a correlation receiver, as in [49], the correlation between $s_{LOS}(f)$ and $s_M(f)$ is examined, as in [50], to study the influence of $s_M(f)$ on the distance estimation, thereby yielding

$$|\text{Corr}_{TOA}| = \frac{1}{B} \left| \int_{f_0 - B/2}^{f_0 + B/2} s_{LOS}(f)^* s_M(f) df \right|$$
$$= \left| \text{sinc}\left(\frac{B}{c_0} \Delta d \right) \right|, \quad (10)$$

with $\Delta d = d_M - d_B$. Note that $|A_{LOS}| = |A_M| = 1$ was assumed to reduce the notational complexity. Hence, for small distance differences Δd, the multipath propagation influences the distance estimation. Because of the multipath propagation's causality, that is $\Delta d > 0$, the distance is systematically estimated to high, as in [2], [7]. Here, UWB systems seek to maximize the bandwidth B, thereby enabling the separation of the LOS from the multipath propagation.

Similar to the TOA analysis, the influence of the multipath propagation on a PDOA system is discussed below. Here, the received signal, with the LOS impinging from angle $\vartheta = 0$, is evaluated at different antenna positions $l_R \in [-L_R/2, L_R/2]$, yielding

$$s_R(l_R) = s_{LOS}(l_R) + s_M(l_R)$$
$$= A_{LOS} e^{-j2\pi f_0 \frac{\sqrt{l_R^2 + d_B^2}}{c_0}} + A_M e^{-j2\pi f_0 \frac{\sin(\vartheta_M) l_R}{c_0}}. \quad (11)$$

Again, the correlation of $s_{LOS}(l_R)$ and $s_M(l_R)$ is used to study the influence of the multipath propagation on the localization
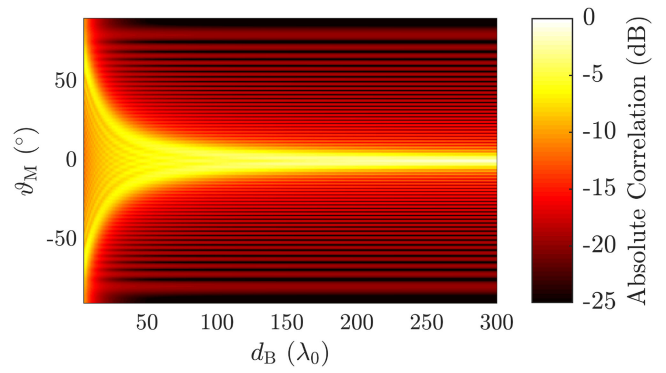

FIGURE 5. Absolute correlation $|\text{Corr}_{PDOA}|$ of the receiving signal of a beacon, located in front of an array with size $L_R = 30\lambda_0$ at distance d_B, and a plane wave coming from ϑ_M.

accuracy. This yields

$$|\text{Corr}_{PDOA}| = \frac{1}{L_R} \left| \int_{-L_R/2}^{L_R/2} s_{LOS}(l_R)^* s_M(l_R) dl_R \right|$$
$$= \frac{1}{L_R} \left| \int_{-L_R/2}^{L_R/2} e^{-j\frac{2\pi}{\lambda_0}\left(\sqrt{l_R^2 + d_B^2} - \sin(\vartheta_M) l_R\right)} dl_R \right|, \quad (12)$$

with $\lambda_0 = c_0/f_0$. Generally, (12) is not solvable in closed form. However, assuming the far field condition $d_B \gg L_R$ as a special case, (12) reduces to

$$|\text{Corr}_{PDOA}| \overset{d_B \gg L_R}{=} \frac{1}{L_R} \left| \int_{-L_R/2}^{L_R/2} e^{j\frac{2\pi}{\lambda_0}\sin(\vartheta_M) l_R} dl_R \right|$$
$$= \left| \text{sinc}\left(\frac{L_R}{\lambda_0} \sin(\vartheta_M) \right) \right|. \quad (13)$$

Hence, similar to TOA systems, where the correlation decreases for high distance differences, in PDOA systems, the correlation decreases for high angle differences. Thus, in the far field domain, multipath propagation strongly distorts the localization, whenever the multipath wave impinges from an only slightly different direction than the LOS, such as reflections on the ground, as in [51]. Unlike TOA systems, the multipath can distort the position estimation toward all directions, depending on the direction of the impinging wave, as in [7]. In order to increase a receiver's capability to separate the LOS from the multipath, large arrays are useful. However, large arrays in indoor environments will not operate under far field conditions and, therefore, an analysis of (12) in the array's near field is necessary. Since (12) cannot be solved in closed form, its behavior will be studied in a heuristic manner. For this purpose, Fig. 5 depicts the correlation (12) for an array of size $L_R = 30\lambda_0$ depending on the distance of the beacon. As expected, for large d_B the sinc($\cdot$) function in (13) appears, as the far-field condition is met. For small beacon distances, the absolute correlation is spread over the entire angular range. On the one hand, this implies that impinging waves from all directions distort the localization process. On the other hand, the influence of strong reflectors, as the ground in [51], is
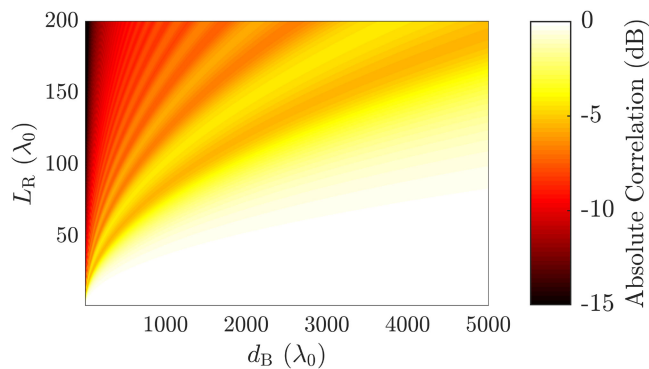
FIGURE 6. Absolute correlation $|\text{Corr}_{\text{PDOA}}|$ of the receiving signal of a beacon, located in front of an array with size L_R at distance d_B, and a plane wave coming from behind the beacon.

reduced. Further, the influence varies for small beacon movements, which can be well utilized in recursive filters. Overall, the impact of multipath propagation on the localization process is reduced. From Fig. 5, it can also be concluded that the absolute correlation behavior can be well approximated by inspecting the correlation for $\vartheta_M = 0$. Therefore, Fig. 6 depicts the correlation for $\vartheta_M = 0$ for different array sizes, L_R, and beacon distances, d_B. Because of the nonlinear phase behavior of circular waves, particularly for very large arrays, the LOS and the multipath propagation can be well decorrelated even for large beacon distances. Note that the correlation was evaluated for an array, which continuously evaluates the receive signal over the array size. Hence, the behavior will vary for sparse arrays, as in [24].

IV. DISCUSSION ON THE IMPLICATIONS FOR 3D INDOOR LOCALIZATION

Thus far, TOA and PDOA measurements have been compared for single measurements. While TOA systems evaluate frequency-dependent phase differences, PDOA systems evaluate position-dependent phase differences. Hence, both approaches follow fairly similar measurement concepts. Since the measurement sensitivity of PDOA systems is particularly high for beacons located close to the receiver, as discussed in Section II, they are very suitable for indoor localization systems. Thereby, assuming the two localization concepts to operate at the same center frequency, f_0, the PDOA system outperforms the TOA system whenever the relative aperture size L_R/d_{max} is higher than the relative bandwidth B/f_0. Hence, the design goal is to increase the size of the receiver to the fullest extent possible. As discussed in Section III, these large arrays also enable the suppression of the effects of multipath propagation, which is commonly considered the main problem for indoor localization systems [2]. This effect is similarly valid for moving receivers or transmitters, thereby creating a synthetic aperture, which can is examined in [51]. Note that the same effect also enables the in-situ calibration of antenna arrays in indoor localization systems, as in [52].

To combine the information of several receivers, typically recursive filters are used for sensor fusion and the incorporation of the beacon movement statistics [7], [16], [38], [51], [53], [54]. For this purpose, the measurement error statistics must be modeled as precisely as possible. Commonly, the measurement errors are modeled zero-mean, normally distributed, and uncorrelated both between the receiving units and for different time instances. Here, especially biased measurements automatically result in biased estimations [55]. Hence, the TOA measurements, which are impaired by a distance offset due to multipath, as well documented for different UWB systems in [7], depict a strong challenge for 3D localization. Further, antenna modeling issues further deteriorate the localization results, which can barely be modeled zero mean and uncorrelated. In contrast, the multipath propagation can impinge from arbitrary directions and, hence, their influence is bias-free in rich scattering environments. However, even for multipath propagation with a single dominant reflection, for example the ground in [51], the influence of the multipath propagation can be decreased by increasing the aperture size. In addition, PDOA receivers are easy to implement using small narrow band antennas that provide high directional coverage with almost constant radiation patterns. Hence, PDOA systems provide measurements that are extremely sensitive to beacon position changes and are affected by errors, which can be assumed to be zero mean for rich scattering conditions and are far less correlated, thereby providing appropriate conditions for 3D position estimation.

The discussed localization principles require different levels of synchronization exactness. Since TOA systems estimate the distance by measuring the time between the transmission and reception of a wave, which translates to the distance estimation via the speed of light, the tolerable timing synchronization error $t_{\text{sync,TOA}}$ is restricted to

$$t_{\text{sync,TOA}} \ll \frac{\sigma_p}{c_0}, \tag{14}$$

where σ_p represents the position deviation due to other impairments as noise or multipath propagation. The most accurate UWB systems localization systems [12], [13] achieve an accuracy of several millimeters and, hence, the timing errors are restricted to some picoseconds. In a TDOA localization system, only the receivers have to be synchronized to that extend, which is still very challenging [12]. Since in narrow band systems small timing errors directly translate to phase changes between each beacon–receiver pair, but do not affect their phase difference measurement itself, the PDOA evaluation is fairly resistant against synchronization errors. Therefore, it is sufficient to synchronize the receivers such that the position variation of the beacon within the maximal timing error is less than the position deviation σ_p. Thus, the timing synchronization error should satisfy

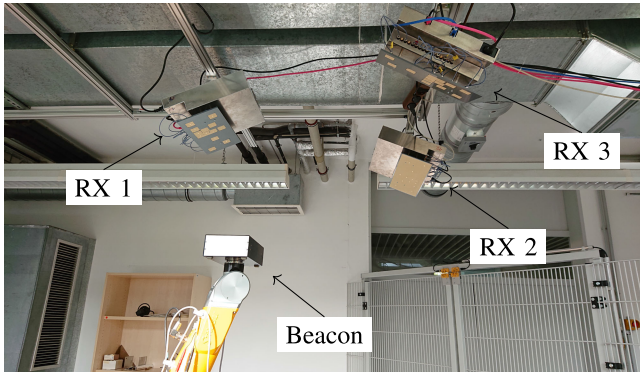$$t_{\text{sync,PDOA}} \ll \frac{\sigma_p}{v_{B,\text{max}}}, \tag{15}$$

FIGURE 7. Illustration of the measurement setup, which comprises three receivers and one beacon.

where $v_{B,max}$ denotes the maximal beacon speed. Hence, timing errors up to 1 ms can be tolerated within typical measurement conditions to achieve a localization accuracy of several millimeters. Furthermore, the evaluated narrow band signals can be arbitrarily modulated, because only relative phases are evaluated. Thus, PDOA systems can be easily implemented within established communication standards, for example Bluetooth or wireless local area network (WLAN). The most promising application of PDOA-based localization is mobile radio communication, particularly in terms of 5G [33], [34] and 6G [56], [57], which is used both outdoors and indoors to enable high data rates in user hotspots [33]. Here, MMIMO systems drastically increase the number of antennas of the base station [37], [58], enabling very high data rate by improving the spatial diversity of the base station [59]. In doing so, MMIMO communication systems avoid the excessive usage of bandwidth by increasing the number of receive antennas and, thus, represent a direct counterpart of the analogy between bandwidth and aperture size for localization systems in Section II.

V. EXPERIMENTAL VERIFICATION

To demonstrate the feasibility of PDOA systems for indoor localization, a 24 GHz CW beacon is localized within the measurement setup, as depicted in Fig. 7. Note that the environment depicts a challenging multipath scenario with a closely spaced metallic fence and reflecting walls. To localize the beacon, three receiver arrays of size 25.4 cm × 9.1 cm ≈ $20.3 \lambda_0 \times 7.3 \lambda_0$ are available. The beacon is mounted on a highly accurate robotic arm, which can be moved within a cubic area under the arrays with edges of approximately 1 m. Although the localization area is less than the size of a standard room, the results are easily transferable to a bigger room using larger arrays. However, the limited area is selected because of the availability of the highly accurate robotic arm, which enables the localization verification. Evaluating the equivalent bandwidth in (7) with $d_{max} = 1$ m and the longer array side as L_R yields $B_{PDOA,eq} \approx 6.1$ GHz, which lies within

the area of the available bandwidth in the UWB band 3.1 GHz-10.6 GHz and, therefore, the PDOA localization result can be well compared to UWB localization results from literature.

A. HOLOGRAPHIC EXTENDED KALMAN FILTER

Generally, an efficient evaluation of spatially distributed phases is difficult because of their ambiguity. The most established processing method of spatially distributed phase measurements estimates the AOAs at each receiver [20], thereby providing unambiguous directional information. Then, the AOA estimations of several receivers can be combined via multiangulation, for example using an EKF [60]. Unfortunately, the AOA estimation limits the achievable localization accuracy, mainly because of two reasons. First, the AOA estimation depicts a nonlinear preprocessing, which sporadically yields high angle estimation errors [30], particularly under multipath conditions [51]. The resulting error statistics are no more normally distributed with known, constant variance and, hence, are not suited for typical least square estimators as the EKF [55]. Second, the AOA estimation requires the incident wave to be plane and, consequently, the size of the receiver arrays is limited. However, to enable highly accurate PDOA-based indoor localization, large receiver arrays are necessary, which provide high measurement sensitivity and reduce the influence of multipath propagation, as discussed in Sections II and III, respectively. In order to use large receiver arrays and to avoid ambiguity issues, the HEKF, proposed in [38], directly evaluates the phase differences in a recursive predict-update manner without further preprocessing. Hence, the HEKF avoids large angle estimation errors, because the current beacon position is estimated by a direct phase difference evaluation in the surrounding of the previous beacon position, and implicitly profits from the multipath decorrelation effect in Section III. Though the HEKF was already proposed in [38], it is presented here for completeness. The HEKF evaluates the phase differences of N_R receivers, where the n_Rth array contains N_{A,n_R} receive antennas, in a recursive manner. In the respective measurement setup used for validation in this work and presented in Fig. 7, $N_R = 3$ receivers, each evaluating $N_{A,n_R} = 12$ antennas, are used. Hence, at each array, a measurement vector $\bar{y}_{n_R,k}^{meas}$ consisting of N_{A,n_R} phase measurements

$$\varphi_{n_R,n_A,k} = -2\pi \frac{f_0}{c_0} d_{n_R,n_A,k} + \Delta\varphi_{n_R,k} \qquad (16)$$

exists, where $d_{n_R,n_A,k}$ denotes the distance between the beacon and the n_Ath antenna of the n_Rth receiver and $\Delta\varphi_{n_R,k}$ denotes the unknown phase difference between the beacon and the n_Rth receiver in the kth sample. By stacking the measured phases at all receivers, the complete measurement vector $\bar{y}_k^{meas}$, which contains all absolute phases, is constructed. To eliminate the unknown phases $\Delta\varphi_{n_R,k}$, the preprocessing matrix D calculates $N_{A,n_R} - 1$ phase differences at each receiver as

$$\bar{y}_{\Delta,k}^{meas} = \mathrm{mod}'_{2\pi}\left(D\bar{y}_k^{meas}\right), \qquad (17)$$

Algorithm 1: Holographic Extended Kalman Filter.

1. Prediction:

$$\vec{x}_{k|k-1} = \boldsymbol{F}\vec{x}_{k-1|k-1}$$

$$\boldsymbol{P}_{k|k-1} = \boldsymbol{F}\boldsymbol{P}_{k-1|k-1}\boldsymbol{F}^{\mathrm{T}} + \sigma_{\mathrm{vel}}^{2}\boldsymbol{G}\boldsymbol{G}^{\mathrm{T}}$$

2. Update:

$$\vec{y}_{\Delta,k}^{\mathrm{meas}} = \boldsymbol{D}\vec{y}_{k}^{\mathrm{meas}}$$

$$\vec{d}(\vec{x}_{k|k-1}) = \mathrm{mod}_{2\pi}' \left(\vec{y}_{\Delta,k}^{\mathrm{meas}} - \vec{h}_{\Delta}(\vec{x}_{k|k-1}) \right)$$

$$\boldsymbol{H}_k = \left. \frac{\partial \vec{h}_{\Delta}(\vec{x}_k)}{\partial \vec{x}_k} \right|_{\vec{x}_{k|k-1}}$$

$$\boldsymbol{K}_k = \boldsymbol{P}_{k|k-1}\boldsymbol{H}_k^{\mathrm{T}} \left(\boldsymbol{H}_k\boldsymbol{P}_{k|k-1}\boldsymbol{H}_k^{\mathrm{T}} + \boldsymbol{R}_{\Delta} \right)^{-1}$$

$$\vec{x}_{k|k} = \vec{x}_{k|k-1} + \boldsymbol{K}_k\vec{d}(\vec{x}_{k|k-1})$$

$$\boldsymbol{P}_{k|k} = (\boldsymbol{I} - \boldsymbol{K}_k\boldsymbol{H}_k)\boldsymbol{P}_{k|k-1}$$

where $\mathrm{mod}_{2\pi}'(\cdot)$ maps the ambiguous phases to $(-\pi, \pi]$, as in (1). To evaluate the phase differences in a Kalman filter-based manner, a constant velocity model with a state vector $\vec{x}_k = [p_{x,k}, p_{y,k}, p_{z,k}, v_{x,k}, v_{y,k}, v_{z,k}]$, containing the position and velocity of the beacon, is assumed. Hence, the state transition function is given by

$$\vec{x}_k = \boldsymbol{F}\vec{x}_{k-1} + \boldsymbol{G}\vec{\omega}_{\mathrm{vel},k}, \tag{18}$$

where $\boldsymbol{F}$ represents the constant velocity model's state transition and $\vec{\omega}_{\mathrm{vel},k} \sim \mathcal{N}(0, \sigma_{\mathrm{vel}}^2\boldsymbol{I})$ is the velocity noise, which is mapped onto velocity and position changes using $\boldsymbol{G}$, as in [38]. To compare the measured phase differences with hypothetical phase differences, the measurement is defined as

$$\vec{y}_k = \boldsymbol{D}(\vec{h}(\vec{x}_k) + \vec{n}_k)$$

$$= \boldsymbol{D}\vec{h}(\vec{x}_k) + \boldsymbol{D}\vec{n}_k$$

$$= \vec{h}_{\Delta}(\vec{x}_k) + \boldsymbol{D}\vec{n}_k, \tag{19}$$

where $\vec{h}(\vec{x}_k)$ models the absolute phases, as in (16), $\vec{h}_{\Delta}(\vec{x}_k) = \boldsymbol{D}\vec{h}(\vec{x}_k)$ evaluates the hypothetical phase differences as in (17), and $\vec{n}_k \sim \mathcal{N}(0, \sigma_{\varphi}^2\boldsymbol{I})$, thereby yielding the phase differences to be corrupted by correlated noise as $\boldsymbol{D}\vec{n}_k \sim \mathcal{N}(0, \boldsymbol{R}_{\Delta} = \sigma_{\varphi}^2\boldsymbol{D}\boldsymbol{D}^{\mathrm{T}})$. Evaluating the phase difference measurements in an extended Kalman filter-based manner [32] yields the HEKF, which is presented in Algorithm 1. Note that here, the $\mathrm{mod}_{2\pi}'(\cdot)$ function from (1) is only applied in the final error calculation to map the difference $\vec{d}(\vec{x}_{k|k-1})$ between the prediction and the measurement to $(-\pi, \pi]$. Hence, the update rate must be sufficiently high such that the absolute phase differences are considerably less than π between successive measurements.
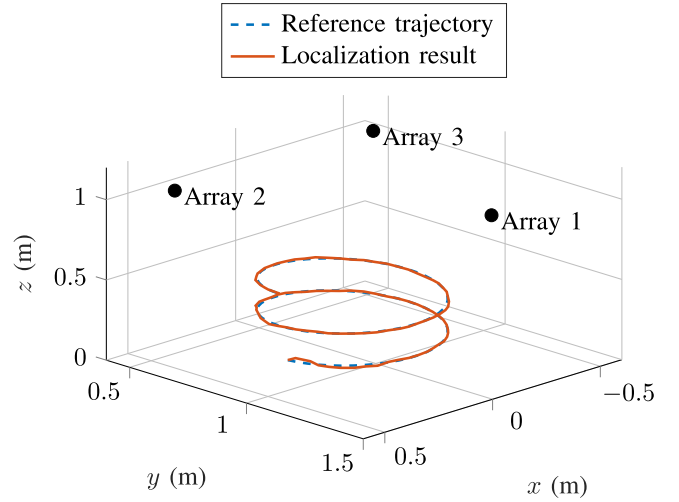

FIGURE 8. Localization result of a 24 GHz beacon, which drives a helix trajectory, using three antenna arrays, each containing 12 antennas, within the measurement setup depicted in Fig. 7.
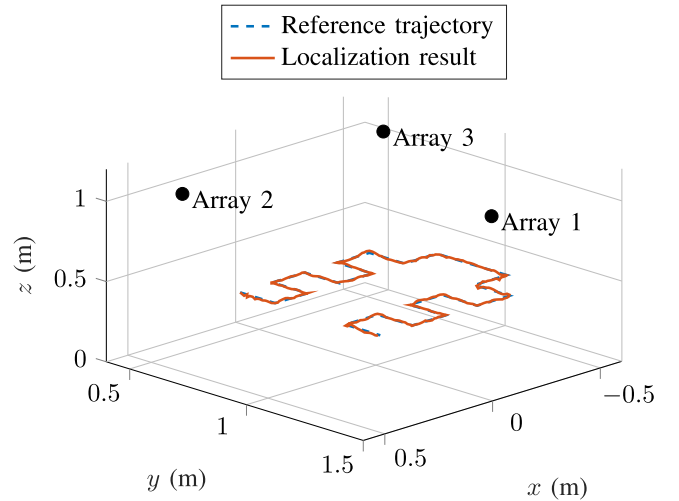

FIGURE 9. Localization result of a 24 GHz beacon, which drives a trajectory consisting of several straight lines, using three antenna arrays, each containing 12 antennas, within the measurement setup depicted in Fig. 7.

B. MEASUREMENT RESULTS

To evaluate the PDOA localization capabilities, the antenna arrays in Fig. 7 have been calibrated using the algorithm in [52]. Then, the helix trajectory in Fig. 8, consisting of 100 successive beacon positions, and the trajectory in Fig. 9, consisting of 330 successive beacon positions, were driven by the robotic arm. At every position, each array performed an individual measurement, which is then used for the HEKF-based localization. Evaluating the localization results yields a position root mean square error (RMSE) of 5.3 mm for the helix trajectory and 4.8 mm for the trajectory in Fig. 9, when the constant velocity model of the Kalman filter is activated. The pure PDOA localization is evaluated by deactivating the Kalman filter's constant velocity model, that is $\sigma_{\mathrm{vel}}^2 \to \infty$,

TABLE 1. Comparison With 3D UWB Localization Results

Publication	Technique	B	$B_{\mathrm{PDOA,eq}}$	Error
This work	PDOA	$\approx 0\,\mathrm{GHz}$ (CW)	$\approx 6.1\,\mathrm{GHz}$	4-6 mm
[12]	TDOA	$>3\,\mathrm{GHz}$	$\doteq B$	2-4 mm
[13]	TDOA	$5.2\,\mathrm{GHz}$	$\doteq B$	2-5 mm
[14]	TOA	$7\,\mathrm{GHz}$	$\doteq B$	1-2 cm
[15]	TOA	$0.5\,\mathrm{GHz}$	$\doteq B$	11 cm
[16]	TOA	$0.9\,\mathrm{GHz}$	$\doteq B$	20 cm
[7]	TOA	$0.9\,\mathrm{GHz}$	$\doteq B$	59 cm

thereby yielding a RMSE of 5.8 mm for the helix trajectory and 5.3 mm for the trajectory in Fig. 9. Here, the localization accuracy of the helix trajectory is slightly worse, which can be explained by the higher average distance between the beacon and the receivers.

Table 1 presents the localization errors and bandwidths of different 3D UWB localization systems in literature, thereby enabling a direct comparison with the presented PDOA localization results via the equivalent bandwidth $B_{\mathrm{PDOA,eq}}$. Note that only 3D localization results are listed here. However, [10] provides a broad overview for different UWB topics. Generally, a fair comparison is very difficult because of the strongly varying measurement setups, including multipath conditions and the 3D sizes of the measurement areas. The results in Table 1 can be divided into two groups, one group [12]–[14] with localization errors of approximately 1 cm and one group [7], [15], [16] with errors of over 10 cm, which can easily be explained via the used bandwidth of several GHz or less than one GHz, respectively. In addition to the higher bandwidth, it is noticeable that all publications of the first group [12]–[14] vary the transmitter height only very little. This is reasoned in modeling problems of the transmit and receive antennas of TOA localization systems with very high relative bandwidths, as discussed in Section II. In particular, the publications [12], [13], which provide outstanding localization results, used monopole antennas as transmitters, which can provide a constant behaviour in horizontal direction. However, large height changes or transmitter rotations and, hence, a practical 3D localization is not possible. Further, the measurements are conducted in low multipath environments, particularly in [12] that used an anechoic chamber. Thus, although the results are impressive, they cannot be easily translated into a general indoor 3D localization scheme, particularly regarding the localization of consumer devices.

In comparison, the depicted indoor PDOA measurements with an equivalent bandwidth $B_{\mathrm{PDOA,eq}} \approx 6.1$ GHz in the range of the UWB bandwidths of the exact group [12]–[14] provides similar localization results, although the measurements were conducted in a severe multipath environment. Further, the transmitter can be freely moved in all directions, because narrow band patch antennas with an almost constant behavior for different directions are used. To enable similar localization results in a larger area, the receiver array's size can easily be increased, thereby providing the same measurement sensitivity with higher beacon-receiver distances, while the multipath suppression capability is further improved, as discussed in Section III.

VI. CONCLUSION

In this paper, a basic comparison between TOA and PDOA systems has been presented. In doing so, the similarity between bandwidth and aperture size was depicted, thereby proposing to focus future research on the implementation of physically large PDOA systems to advance indoor localization. This will enable accurate positioning within current and future communication standards without adopting their devices. In this process, the incorporation of additional sensors like inertial measurement units that are commonly available, enables further improvements. A key challenge for the utilization of PDOA in 5G and 6 G depicts the necessity for array calibration, which has to be performed during receiver installation and perhaps refreshed regularly. Hence, it is necessary to conduct future research on sophisticated calibration methods that can cope with challenging environments without excessive measurements.

REFERENCES

[1] R. Mautz, "Indoor positioning technologies," Dept Civil, Environ. Geomatic Eng., ETH Zurich, Zurich, Switzerland, 2012.

[2] S. Aditya, A. F. Molisch, and H. M. Behairy, "A survey on the impact of multipath on wideband time-of-arrival based localization," *Proc. IEEE Proc. IRE*, vol. 106, no. 7, pp. 1183–1203, Jul. 2018.

[3] I. Ashraf, S. Hur, and Y. Park, "Smartphone sensor based indoor positioning: Current status, opportunities, and future challenges," *Electronics*, vol. 9, no. 6, Jun. 2020, Art. no. 891.

[4] M. Vossiek, L. Wiebking, P. Gulden, J. Wieghardt, C. Hoffmann, and P. Heide, "Wireless local positioning," *IEEE Microw. Mag.*, vol. 4, no. 4, pp. 77–86, Dec. 2003.

[5] M. Chen, A. Xia, and Y. Zeng, "Analysis of multipath effects on accuracy of range estimation using received signal strength indicator," in *Proc. 4th Int. Conf. Commun. Syst. Netw. Technol.*, Apr. 2014, pp. 314–316.

[6] S. Roehr, P. Gulden, and M. Vossiek, "Method for high precision clock synchronization in wireless systems with application to radio navigation," in *Proc. IEEE Radio Wireless Symp.*, Jan. 2007, pp. 551–554.

[7] A. R. J. Ruiz and F. S. Granja, "Comparing ubisense, BeSpoon, and DecaWave UWB location systems: Indoor performance analysis," *IEEE Trans. Instrum. Meas.*, vol. 66, no. 8, pp. 2106–2117, Aug. 2017.

[8] P. Scherz, A. Haderer, R. Feger, G. Stelzhammer, and A. Stelzer, "Array processing system for the local position measurement system LPM," in *Proc. Conf. ICECom, 20th Int. Conf. Appl. Electromagnetics Commun.*, Sep. 2010, pp. 1–4.

[9] L. Zwirello, T. Schipper, M. Jalilvand, and T. Zwick, "Realization limits of impulse-based localization system for large-scale indoor applications," *IEEE Trans. Instrum. Meas.*, vol. 64, no. 1, pp. 39–51, Jan. 2015.

[10] A. Alarifi *et al.*, "Ultra wideband indoor positioning technologies: Analysis and recent advances," *Sensors*, vol. 16, no. 5, May 2016, Art. no. 707.

[11] S. Gezici *et al.*, "Localization via ultra-wideband radios: A look at positioning aspects for future sensor networks," *IEEE Signal Process. Mag.*, vol. 22, no. 4, pp. 70–84, Jul. 2005.

[12] M. R. Mahfouz, C. Zhang, B. C. Merkl, M. J. Kuhn, and A. E. Fathy, "Investigation of high-accuracy indoor 3-D positioning using UWB technology," *IEEE Trans. Microw. Theory Techn.*, vol. 56, no. 6, pp. 1316–1330, Jun. 2008.

[13] C. Zhang, M. J. Kuhn, B. C. Merkl, A. E. Fathy, and M. R. Mahfouz, "Real-time noncoherent UWB positioning radar with millimeter range accuracy: Theory and experiment," *IEEE Trans. Microw. Theory Techn.*, vol. 58, no. 1, pp. 9–20, Jan. 2010.

[14] R. Bharadwaj, C. Parini, and A. Alomainy, "Experimental investigation of 3-D human body localization using wearable ultra-wideband antennas," *IEEE Trans. Antennas Propag.*, vol. 63, no. 11, pp. 5035–5044, Nov. 2015.

[15] B. Silva, Z. Pang, J. Åkerberg, J. Neander, and G. Hancke, "Experimental study of UWB-based high precision localization for industrial applications," in *Proc. IEEE Int. Conf. Ultra-WideBand*, Sep. 2014, pp. 280–285.

[16] M. Ridolfi *et al.*, "Experimental evaluation of UWB indoor positioning for sport postures," *Sensors*, vol. 18, no. 1, Jan. 2018, Art. no. 168.

[17] A. Richard Thompson, J. M. Moran, and G. W. Swenson, Jr., *Interferometry and Synthesis in Radio Astronomy*. Cham, Switzerland: Springer Nature, 2017.

[18] R. M. Goldstein, H. A. Zebker, and C. L. Werner, "Satellite radar interferometry: Two-dimensional phase unwrapping," *Radio Sci.*, vol. 23, no. 4, pp. 713–720, Jul. 1988.

[19] R. Bamler and P. Hartl, "Synthetic aperture radar interferometry," *Inverse Problems*, vol. 14, no. 4, pp. R1–R54, Aug. 1998.

[20] H. L. V. Trees, *Optimum Array Processing: Part IV of Detection, Estimation, and Modulation Theory*. Hoboken, NJ, USA: Wiley, 2004.

[21] C. E. Konig and W. Skudera, "Angle of arrival phase interferometer direction finding system." Tech. Rep., DELEW-TR-82-1, Electron. Warfare Lab., U.S. Army Electron. Res. Devel. Command, Fort Monmouth, NJ, USA, 1982.

[22] L. Balogh and I. Kollar, "Angle of arrival estimation based on interferometer principle," in *Proc. IEEE Int. Symp. Intell. Signal Process.*, Sep. 2003, pp. 219–223.

[23] I. Amundson, J. Sallai, X. Koutsoukos, and A. Ledeczi, "Radio interferometric angle of arrival estimation," in *Wireless Sensor Networks*, ser. *Lecture Notes in Computer Science*, J. S. Silva, B. Krishnamachari, and F. Boavida, Eds. Berlin Germany: Springer, 2010, pp. 1–16.

[24] T. Pavlenko, C. Reustle, Y. Dobrev, M. Gottinger, L. Jassoume, and M. Vossiek, "Design and optimization of sparse planar antenna arrays for wireless 3-D local positioning systems," *IEEE Trans. Antennas Propag.*, vol. 65, no. 12, pp. 7288–7297, Dec. 2017.

[25] J. N. Ash and L. C. Potter, "Robust system multiangulation using subspace methods," in *Proc. 6th Int. Symp. Inf. Process. Sensor Netw.*, Apr. 2007, pp. 61–68.

[26] A. Dempster, "Dilution of precision in angle-of-arrival positioning systems," *Electron. Lett.*, vol. 42, no. 5, pp. 291–292, Mar. 2006.

[27] X. Lv, K. Liu, and P. Hu, "Geometry influence on GDOP in TOA and AOA positioning systems," in *Proc. 2nd Int. Conf. Netw. Secur., Wireless Commun. Trusted Comput.*, vol. 2, Apr. 2010, pp. 58–61.

[28] M. Gavish and A. J. Weiss, "Performance analysis of bearing-only target location algorithms," *IEEE Trans. Aerosp. Electron. Syst.*, vol. 28, no. 3, pp. 817–828, Jul. 1992.

[29] S. Ravindra and S. N. Jagadeesha, "Time of arrival based localization in wireless sensor networks: A linear approach," 2014, *arXiv:1403.6697*.

[30] M. Hehn, E. Sippel, and M. Vossiek, "An iterative extended kalman filter for coherent measurements of incoherent network nodes in positioning systems," *IEEE Access*, vol. 8, pp. 36 714–36 727, 2020.

[31] Y. Bar-Shalom, X.-R. Li, and T. Kirubarajan, *Estimation With Applications to Tracking and Navigation*. Hoboken, NJ, USA: Wiley, Inc., 2001.

[32] S. Thrun, W. Burgard, and D. Fox, *Probabilistic Robotics, Ser. Intelligent Robotics and Autonomous Agents*. Cambridge, MA, USA: MIT Press, 2005.

[33] V. Jungnickel *et al.*, "The role of small cells, coordinated multipoint, and massive MIMO in 5G," *IEEE Commun. Mag.*, vol. 52, no. 5, pp. 44–51, May 2014.

[34] P. Gröschel *et al.*, "An ultra-versatile massive MIMO transceiver testbed for multi-Gb/s communication," in *Proc. IEEE 2nd 5G World Forum*, Sep. 2019, pp. 1–6.

[35] I. F. Akyildiz, A. Kak, and S. Nie, "6G and beyond: The future of wireless communications systems," *IEEE Access*, vol. 8, pp. 133 995–134 030, 2020.

[36] S. Zhang, C. Xiang, and S. Xu, "6G: Connecting everything by 1000 times price reduction," *IEEE Open J. Veh. Technol.*, vol. 1, pp. 107–115, 2020.

[37] Z. Zhang *et al.*, "6G wireless networks: Vision, requirements, architecture, and key technologies," *IEEE Veh. Technol. Mag.*, vol. 14, no. 3, pp. 28–41, Sep. 2019.

[38] M. Lipka, E. Sippel, and M. Vossiek, "An extended kalman filter for direct, real-time, phase-based high precision indoor localization," *IEEE Access*, pp. 1–10, 2019.

[39] W. L. Stutzman and G. A. Thiele, *Antenna Theory and Design*. Hoboken, NJ, USA: Wiley, 1981.

[40] C. A. Balanis, *Antenna Theory: Analysis and Design*. Hoboken, NJ, USA: Wiley, 2012.

[41] L. J. Chu, "Physical limitations of omni-directional antennas," *J. Appl. Phys.*, vol. 19, no. 12, pp. 1163–1175, Dec. 1948.

[42] H. Wheeler, "Small antennas," *IEEE Trans. Antennas Propag.*, vol. 23, no. 4, pp. 462–469, Jul. 1975.

[43] W. Davis, T. Yang, E. Caswell, and W. Stutzman, "Fundamental Limits on Antenna Size: A. new Limit," *IET Microw. Antennas Propag.*, vol. 5, no. 11, pp. 1297–1302, Aug. 2011.

[44] R. Cicchetti, E. Miozzi, and O. Testa, "Wideband and UWB antennas for wireless applications: A comprehensive review," *Int. J. Antennas Propag.* vol. 2017, 2017, Art no. e2390808. [Online]. Available: https://www.hindawi.com/journals/ijap/2017/2390808/

[45] U. Schwarz, V. Zhukov, R. Stephan, and M. A. Hein, "Determination of phase centers of ultra-wideband antennas," in *Proc. 4th Eur. Conf. Antennas Propag.*, Apr. 2010, pp. 1–4.

[46] M. El-Hadidy and T. Kaiser, "Impact of ultra wide-band antennas on communications in a spatial cannel," in *Proc. 1st Int. Conf. Cogn. Radio Oriented Wireless Netw. Commun.*, Jun. 2006, pp. 1–5.

[47] Y. Duroc, A. Ghiotto, T. P. Vuong, and S. Tedjini, "UWB antennas: Systems with transfer function and impulse response," *IEEE Trans. Antennas Propag.*, vol. 55, no. 5, pp. 1449–1451, May 2007.

[48] Q. Spencer, B. Jeffs, M. Jensen, and A. Swindlehurst, "Modeling the statistical time and angle of arrival characteristics of an indoor multipath channel," *IEEE J. Sel. Areas Commun.*, vol. 18, no. 3, pp. 347–360, Mar. 2000.

[49] T. Callaghan, N. Czink, F. Mani, A. Paulraj, and G. Papanicolaou, "Correlation-based radio localization in an indoor environment," *EURASIP J. Wireless Commun. Netw.*, vol. 2011, no. 1, Oct. 2011, Art. no. 135.

[50] P. D. Teal, T. D. Abhayapala, and R. A. Kennedy, "Spatial correlation for general distributions of scatterers," *IEEE Signal Process. Lett.*, vol. 9, no. 10, pp. 305–308, Oct. 2002.

[51] J. Geiß, E. Sippel, P. Gröschel, M. Hehn, and M. Vossiek, "A wireless local positioning system concept and 6D localization approach for cooperative robot swarms based on distance and angle measurements," *IEEE Access*, vol. 8, pp. 115 501–115 514, 2020.

[52] E. Sippel, M. Lipka, J. Geiß, M. Hehn, and M. Vossiek, "In-situ calibration of antenna arrays within wireless locating systems," *IEEE Trans. Antennas Propag.*, vol. 68, no. 4, pp. 2832–2841, Apr. 2020.

[53] E. Choi and S. Chang, "An adaptive tracking estimator for robust vehicular localization in shadowing areas," *IEEE Access*, vol. 7, pp. 42 436–42 444, 2019.

[54] V. Djaja-Josko and J. Kolakowski, "Application of kalman filter for positioning precision improvement in UWB localization system," in *Proc. 24th Telecommun. Forum*, Nov. 2016, pp. 1–4.

[55] Kay, *Fundamentals of Statistical Signal Processing*. Vol. 1, *Estimation Theory*. Upper Saddle River, NJ, USA: Prentice-Hall, 1993.

[56] E. Larsson, O. Edfors, F. Tufvesson, and T. Marzetta, "Massive MIMO for next generation wireless systems," *IEEE Commun. Mag.*, vol. 52, no. 2, pp. 186–195, Feb. 2014.

[57] L. Lu, G. Li, A. Swindlehurst, A. Ashikhmin, and R. Zhang, "An overview of massive MIMO: Benefits and challenges," *IEEE J. Sel. Topics Signal Process.*, vol. 8, no. 5, pp. 742–758, Oct. 2014.

[58] J. Hoydis, S. ten Brink, and M. Debbah, "Massive MIMO in the UL/DL of cellular networks: How many antennas do we need?," *IEEE J. Sel. Areas Commun.*, vol. 31, no. 2, pp. 160–171, Feb. 2013.

[59] E. Björnson, E. G. Larsson, and T. L. Marzetta, "Massive MIMO: 10 myths and one grand question," 2015, *arXiv:1503.06854*.

[60] M. Lipka *et al.*, "Wireless 3D localization concept for industrial automation based on a bearings only extended Kalman filter," in *Proc. Asia-Pacific Microw. Conf.*, Nov. 2018, pp. 821–823.

ERIK SIPPEL was born in Fürth, Germany, in 1991. He received the M.Sc. degree in electronic engineering in 2015 from Friedrich-Alexander-Universität Erlangen-Nürnberg (FAU), Erlangen, Germany, where he is currently working toward the Ph.D. degree.

In 2016, he joined the Institute of Microwaves and Photonics, FAU. His current research interests include indoor localization, especially radar for near-field localization, antenna calibration, data transmission, and analog-to-digital conversion.

JOHANNA GEISS (Student Member, IEEE) was born in Lich, Germany, in 1992.

She received the master's degree in electrical engineering in 2017 from Friedrich-Alexander-Universität Erlangen-Nürnberg (FAU), Erlangen, Germany, where she is currently working toward the Ph.D. degree with the Institute of Microwaves and Photonics (LHFT). She is primarily working in the fields of radar-based localization, sensor-fusion, radar signal processing, radar calibration, and ego-motion estimation.

STEFAN BRÜCKNER was born in Kronach, Germany, in 1992. He received the M.Sc. degree in electronic engineering in 2019 form the Friedrich-Alexander-Universität Erlangen-Nürnberg(FAU), Erlangen, Germany where he is currently working toward the Ph.D. degree. In 2019, he joined the Institute of Microwaves and Photonics, FAU. His current research interests include radar for close range applications, indoor positioning, Kalman filter for localization, and signal processing.

PATRICK GRÖSCHEL (Student Member, IEEE) was born in Nuremberg, Germany, in 1990. He received the M.Sc. dregree in electronic engineering in 2016 from Friedrich Alexander Universität (FAU), Erlangen, Germany, where he is currently working toward the Ph.D. degree with FAU, Erlangen. He has joined the Institute of Microwaves and Photonics, FAU in 2016. His research interests include the design and characterization of massive MIMO systems, error calibration and mitigation, communication and localization, and signal processing based on those systems.

MARKUS HEHN (Student Member, IEEE) was born in Bamberg, Germany, in 1987. He received the M.Sc. degree in electrical engineering in 2016 from Friedrich-Alexander-Universität Erlangen-Nürnberg (FAU), Erlangen, Germany, where he is currently working toward the Ph.D. degree.

In 2016, he joined the Institute of Microwaves and Photonics, FAU. His current research interests include radar for near-field localization and localization systems for indoor environment.

MARTIN VOSSIEK (Fellow, IEEE) received the Ph.D. degree from Ruhr-Universität Bochum, Bochum, Germany, in 1996. In 1996, he joined Siemens Corporate Technology, Munich, Germany, where he was the Head of the Microwave Systems Group, from 2000 to 2003. Since 2003, he has been a Full Professor with Clausthal University, Clausthal-Zellerfeld, Germany. Since 2011, he has been the Chair of the Institute of Microwaves and Photonics (LHFT), Friedrich-Alexander-Universität Erlangen-Nürnberg (FAU), Erlangen, Germany. He has authored or coauthored more than 250 articles. His research has led to more than 90 granted patents. His current research interests include radar, transponder, RF identification, communication, and locating systems. Dr. Vossiek has been a Member of Organizing Committees and Technical Program Committees for many international conferences. He is a Member of the German IEEE Microwave Theory and Techniques (MTT)/Antennas and Propagation (AP) Chapter Executive Board and the IEEE MTT-S Technical Coordinating Committees MTT-24, MTT-27 and MTT 29. He was the Founding Chair of the MTT IEEE Technical Coordinating Subcommittee MTT-27 Wireless-Enabled Automotive and Vehicular Application. Martin Vossiek was the recipient of several international awards. For example, recently, he was Awarded the 2019 Microwave Application Award from the IEEE MTT Society (MTT-S). He has served on the Review Boards for numerous technical journals. From 2013 to 2019, he was an Associate Editor for the IEEE TRANSACTIONS ON MTT.